Magnetic-field-assisted stimulated laser cooling in the (1+3)-level atomic system

Deshui Yu and Jingbiao Chen*

Institute of Quantum Electronics, School of Electronics Engineering and Computer Science, Peking University, Beijing 100871, People's Republic of China

(Received 13 September 2006; revised manuscript received 4 January 2007; published 29 August 2007)

The theory of laser cooling assisted by transverse magnetic field $\mathbf{B_t}$ based on the (1+3)-level atomic system is presented. With the additional $\mathbf{B_t}$, atoms could be redistributed among the upper Zeeman sublevels via Larmor precession, and results in large stimulated radiation force and low temperature. Here we consider this cooling model both for broad transition line and narrow line. A Fokker-Planck-type kinetic equation is derived for a broad line. Numerical result shows that the final temperature could be lower than the Doppler limit. For a narrow line, the Monte Carlo approach is applied to simulate the distribution of atoms in the momentum regime and the result shows that most atoms are distributed around zero velocity with width about several $\hbar k/m$.

DOI: 10.1103/PhysRevA.76.023425 PACS number(s): 32.80.Pj, 06.30.Ft, 06.20.−f, 39.30.+w

I. INTRODUCTION

Laser cooling technologies have been widely applied in many areas. Those for alkali-metal atoms have been maturely developed. However, the usual sub-Doppler cooling techniques [1–4] cannot be applied to nondegenerate ground states of even isotope alkaline-earth-metal atoms, which is the main obstacle of further application of alkaline-earth-metal atoms. Such atoms could be cooled by applying the Doppler technique to a narrow line [5–7]. However, since the force adding to atoms by using a narrow line is only several times larger than the gravitation force, the alkaline-earth-metal atoms cannot be cooled in a sufficiently short time and accordingly cannot be steadily trapped in the magnet-optical trap (MOT). Presently, isotope alkaline-earth-metal atoms could be cooled to the recoil temperature by the quenching cooling method [8–10]. However, this cooling method is very complicated experimentally. Furthermore, it is difficult to get an available quenching laser, and the available ones are expensive. Therefore, our work is motivated by the recent experimental efforts on cooling and trapping of alkaline-earth-metal atoms.

Here we investigate a cooling method, combining stimulated light force [11–15] and magnetic-field-induced Larmor precession [16] to cool the (1+3)-level atoms. The magnetic-field-assisted cooling method is not a new idea, and has already been studied by several authors [17–19]. However, in their cases, the atomic ground states are all degenerate. Thus, the atomic temperature could arrive at the sub-Doppler limit, and the magnetic field is only used to select atomic velocities. To our knowledge, the magnetic-field-assisted cooling method to the particular atomic (1+3)-level system has not been applied before. Therefore, our work could be a supplement to the magnetic-field-assisted cooling methods.

In this paper, we first discuss the basic physical process in our cooling method (Sec. II), and then we carefully investigate the light-pressure force and the atomic temperature by numerically calculating the Fokker-Planck-type kinetic equation derived for a broad line (Sec. III). Finally, we simply introduce the application of our cooling method on the narrow line based on the Monte Carlo method in Sec. IV. In the discussion, we have omitted some calculation, all of which could be found in Appendixes A and B.

II. BASIC PHYSICAL PROCESS

In the common two-level system, as shown in Fig. 1(a), the maximum deceleration attainable is limited by the finite spontaneous decay rate of the upper level, because under the saturation of atomic transition, atoms are almost equally distributed between the ground state $|1\rangle$ and the excited state $|2\rangle$ [20]. With the medium field intensity, atoms on state $|2\rangle$

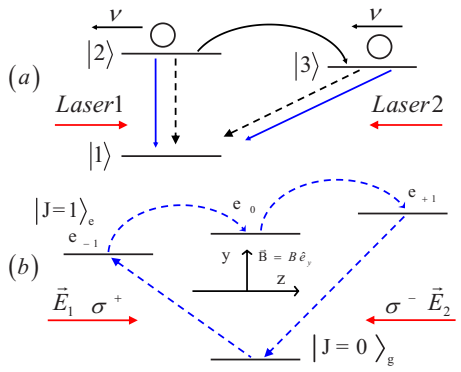

FIG. 1. (Color online) (a) In the two-level atom model, atoms are excited into the upper level $|2\rangle$ by laser 1, and could transit to the ground state $|1\rangle$ by spontaneous decay (dashed line) and stimulated emission (solid line). By using some methods ($\mathbf{B_t}$ induced Larmor precession in this paper) to transfer atoms from state $|2\rangle$ to state $|3\rangle$, which is not coupled with laser 1, atoms could decay to the ground state only by spontaneous emission or stimulated emission caused by laser 2 which couples states $|1\rangle$ and $|3\rangle$. (b) Atoms interact with the laser 1 which has polarization σ^+ traveling along the axis Oz and laser 2 which has polarization σ^- traveling in the opposite direction. Additional transverse static magnetic field $\mathbf{B_t}$ which is along the axis Oy, is used to redistribute the atoms among the Zeeman sublevels of the excited state via Larmor precession.

*jbchen@pku.edu.cn

could scatter photons by both spontaneous emission and stimulated emission. Stimulated emission is a conservative process, which does not change the atomic momentum in average. However, if atoms on state $|2\rangle$ are transferred to another state $|3\rangle$, which is not coupled with the cooling laser 1, atoms could decay to ground state $|1\rangle$ only by spontaneous emission, not the stimulated emission. In this case, the number of atoms participating in the photon scattering will be larger than that of the usual two-level model, and the force will become much larger. In addition, if another field (laser 2), which propagates along the same direction of atomic velocities, couples states $|1\rangle$ and $|3\rangle$, then atoms on state $|3\rangle$ could also transit to ground state $|1\rangle$ by stimulated emission by radiating a photon whose direction is the same as the atomic velocities. As a result, the momentums of the atoms considerably decrease.

In this paper, we consider a one-dimensional scheme of the MOT as shown in Fig. 1(b), of which a (1+3)-level atom interacts with a $\sigma_+ - \sigma_-$ laser field configuration. An additional static magnetic field, $\mathbf{B_t} = \mathcal{B}\mathbf{e_y}$, perpendicular to the quantum axis defined by the laser direction, is introduced to redistribute atoms among the upper Zeeman sublevels. For example, an atom with velocity v along the $\mathbf{z}$ axis is pumped to level $|e_{-1}\rangle$ by laser σ_-, then transfers to level $|e_{+1}\rangle$ via Larmor precession, and finally decays to the ground state by spontaneous emission or by stimulated emission via laser 1 resulting in a large radiation force. In the common Doppler cooling method without $\mathbf{B_t}$, laser 1 only couples $|e_{+1}\rangle - |g_0\rangle$ and laser 2 only couples $|e_{-1}\rangle - |g_0\rangle$. Thus, only the spontaneous emission process could dissipate atomic energy and stimulated emission is a conservative process. However, if we introduce $\mathbf{B_t}$, atoms could be redistributed among Zeeman sublevels via the Larmor precession. Thus, more atoms could decay to ground state by spontaneous emission and stimulated emission. In this case, the stimulated radiated photons propagating along the same direction of atomic velocities result in a much larger radiation pressure force than the case without $\mathbf{B_t}$. This cooling model could be comprehended by another physical process, which will be shown below.

III. BROAD-LINE LASER COOLING

First we consider this cooling method for a broad transition line, for which the probability of spontaneous emission 2γ is larger than one-photon recoil $\hbar k^2/2M$, where M is the mass of the atom. A Fokker-Planck-type kinetic equation is derived for a one-dimension model of a (1+3)-level atom interacting with two counterpropagating circular polarized laser beams and $\mathbf{B_t}$. We numerically discuss the radiation force, diffusion, and temperature.

A. Initial equations

Fields of two counterpropagating laser waves composing a $\sigma^+ - \sigma^-$ field configuration can be written as

$$\mathbf{E}_1 = \tfrac{1}{2}\mathcal{E}(\mathbf{e}_+ e^{i(kz-\omega_l t)} - \mathbf{e}_- e^{-i(kz-\omega_l t)}), \tag{1}$$

$$\mathbf{E}_2 = \tfrac{1}{2}\mathcal{E}(\mathbf{e}_- e^{-i(kz+\omega_l t)} - \mathbf{e}_+ e^{i(kz+\omega_l t)}), \tag{2}$$

where $\mathbf{e}_\pm = \mp \frac{1}{\sqrt{2}}(\mathbf{e}_x \pm i\mathbf{e}_y)$ are the spherical unit vectors, ω_l is the frequency of the cooling laser waves, $k=\omega_l/c$ is the magnitude of the wave vector, and $\mathcal{E}$ is the amplitude of the field. With respect to quantization axis Oz, the first laser wave in Eq. (2) is a σ^+ polarized wave and the second laser wave is a σ^- polarized wave. Since we only consider the temperature in the center of MOT, we can ignore the static inhomogeneous magnetic field, which is introduced to compensate the Doppler frequency shift.

For the above interaction scheme, the atomic Hamiltonian has a standard form

$$H = H_0 - (\hbar^2\nabla^2/2M) - \mathbf{d}\cdot\mathbf{E} - \vec{\mu}\cdot\mathbf{B}, \tag{3}$$

where Hamiltonian H_0 describes the internal atomic states with unperturbed energies E_{g0} and E_{e0}, and Zeeman shifted energies $E_{e,\pm 1}$, and the last two terms describe the electric-dipole and magnetic-dipole interaction between the atom and the fields $\mathbf{E}=\mathbf{E}_1+\mathbf{E}_2$ and $\mathbf{B}=\mathbf{B_t}$. The interaction operators for the atom and fields are as

$$\mathbf{d}\cdot\mathbf{E} = -d_-E_+ + d_0E_0 - d_+E_-,$$

$$\vec{\mu}\cdot\mathbf{B} = -\mu_-B_+ + \mu_0B_0 - \mu_+B_-,$$

where d_α, μ_α, E_α, and B_α with $\alpha=0,\pm$ are the spherical components of the dipole moments and fields.

All the information on the atomic motion in the above fields is included in the density-matrix equation. The density matrix in the Wigner representation is $\rho=\rho(\mathbf{r},\mathbf{p},t)$. The density-matrix elements are defined as

$$\rho_{\alpha\beta}(\mathbf{r},\mathbf{p},t) = \langle\alpha|\rho(\mathbf{r},\mathbf{p},t)|\beta\rangle, \tag{4}$$

where $\alpha,\beta=L,S,J,M_J$ are the quantum numbers of the atomic states. It is convenient to represent the electric field in a form of a plane wave expansion

$$\mathbf{E} = \sum_a \mathbf{E}^a e^{i\mathbf{k_a}\cdot\mathbf{r}-i\omega_l t}. \tag{5}$$

Equations of motion for atomic density matrix elements in the Wigner representation can be expressed as [22]

$$\begin{aligned}
i\hbar\frac{d}{dt}\rho_{kl}(\mathbf{r},\mathbf{p}) = &-\sum_{a,m}\mathbf{d}_{km}\left\{\mathbf{E}^a\rho_{ml}\left(\mathbf{r},\mathbf{p}-\frac{1}{2}\hbar\mathbf{k}_a\right)e^{i\mathbf{k}_a\cdot\mathbf{r}-i(\omega_l-\omega_{km})t}\right.\\
&\left.+\mathbf{E}^{a*}\rho_{ml}\left(\mathbf{r},\mathbf{p}+\frac{1}{2}\hbar\mathbf{k}_a\right)e^{-i\mathbf{k}_a\cdot\mathbf{r}+i(\omega_l-\omega_{mk})t}\right\}\\
&+\sum_{a,n}\mathbf{d}_{nl}\left\{\mathbf{E}^a\rho_{kn}\left(\mathbf{r},\mathbf{p}+\frac{1}{2}\hbar\mathbf{k}_a\right)e^{i\mathbf{k}_a\cdot\mathbf{r}-i(\omega_l-\omega_{nl})t}\right.\\
&\left.+\mathbf{E}^{a*}\rho_{kn}\left(\mathbf{r},\mathbf{p}-\frac{1}{2}\hbar\mathbf{k}_a\right)e^{-i\mathbf{k}_a\cdot\mathbf{r}+i(\omega_l-\omega_{ln})t}\right\}\\
&-\sum_m\vec{\mu}_{km}\cdot\mathbf{B}\rho_{ml}(\mathbf{r},\mathbf{p})+\sum_n\vec{\mu}_{nl}\cdot\mathbf{B}\rho_{kn}(\mathbf{r},\mathbf{p})\\
&-i\hbar\langle k|\Gamma\rho(\mathbf{r},\mathbf{p})|l\rangle,
\end{aligned} \tag{6}$$

where $\frac{d}{dt}=\frac{\partial}{\partial t}+\mathbf{v}\frac{\partial}{\partial\mathbf{r}}$ is the total time derivative, and the quan-

tities $\omega_{ij}=(E_i-E_j)/\hbar$ are assumed to be positive. Here operator Γ describes spontaneous relaxation from the excited-state sublevels $|J_e,M_e\rangle$ to the ground-state level $|J_g=0,M_g=0\rangle$.

In the rotating-wave approximation, all the dynamic equations for the density-matrix elements can be expressed as follows:

$$\frac{d}{dt}\rho_{g_0g_0} = -i\Omega\rho^{(+)}_{g_0e_1}e^{ikz-i\delta t} + i\Omega\rho^{(+)}_{e_1g_0}e^{-ikz+i\delta t} - i\Omega\rho^{(-)}_{g_0e_{-1}}e^{-ikz-i\delta t} + i\Omega\rho^{(-)}_{e_{-1}g_0}e^{ikz+i\delta t} + 2\gamma\langle\rho^{+1}_{e_1e_1}\rangle + 2\gamma\langle\rho^{0}_{e_0e_0}\rangle + 2\gamma\langle\rho^{-1}_{e_{-1}e_{-1}}\rangle,$$

$$\frac{d}{dt}\rho_{e_1e_1} = -2\gamma\rho_{e_1e_1} + i\Omega\rho^{(-)}_{g_0e_1}e^{ikz-i\delta t} - i\Omega\rho^{(-)}_{e_1g_0}e^{-ikz+i\delta t} - \omega_L(\rho_{e_0e_1}+\rho_{e_1e_0}),$$

$$\frac{d}{dt}\rho_{e_0e_0} = -2\gamma\rho_{e_0e_0} + \omega_L(\rho_{e_0e_1}+\rho_{e_1e_0}) - \omega_L(\rho_{e_{-1}e_0}+\rho_{e_0e_{-1}}),$$

$$\frac{d}{dt}\rho_{e_{-1}e_{-1}} = -2\gamma\rho_{e_{-1}e_{-1}} + i\Omega\rho^{(+)}_{g_0e_{-1}}e^{-ikz-i\delta t} - i\Omega\rho^{(+)}_{e_{-1}g_0}e^{ikz+i\delta t} + \omega_L(\rho_{e_{-1}e_0}+\rho_{e_0e_{-1}}),$$

$$\frac{d}{dt}\rho_{g_0e_1} = -\gamma\rho_{g_0e_1} + i\Omega(\rho^{(+)}_{e_1e_1}-\rho^{(-)}_{g_0g_0})e^{-ikz+i\delta t} + i\Omega\rho^{(-)}_{e_{-1}e_1}e^{ikz+i\delta t} - \omega_L\rho_{g_0e_0},$$

$$\frac{d}{dt}\rho_{g_0e_0} = -\gamma\rho_{g_0e_0} + i\Omega\rho^{(+)}_{e_1e_0}e^{-ikz+i\delta t} + i\Omega\rho^{(-)}_{e_{-1}e_0}e^{ikz+i\delta t} + \omega_L(\rho_{g_0e_1}-\rho_{g_0e_{-1}}),$$

$$\frac{d}{dt}\rho_{g_0e_{-1}} = -\gamma\rho_{g_0e_{-1}} + i\Omega(\rho^{(-)}_{e_{-1}e_{-1}}-\rho^{(+)}_{g_0g_0})e^{ikz+i\delta t} + i\Omega\rho^{(+)}_{e_{+1}e_{-1}}e^{-ikz+i\delta t} + \omega_L\rho_{g_0e_0},$$

$$\frac{d}{dt}\rho_{e_{-1}e_0} = -2\gamma\rho_{e_{-1}e_0} + i\Omega\rho^{(+)}_{g_0e_0}e^{-ikz-i\delta t} - \omega_L(\rho_{e_{-1}e_{-1}}-\rho_{e_0e_0}) + \omega_L\rho_{e_{-1}e_1},$$

$$\frac{d}{dt}\rho_{e_0e_1} = -2\gamma\rho_{e_0e_1} - i\Omega\rho^{(-)}_{e_0g_0}e^{-ikz+i\delta t} + \omega_L(\rho_{e_1e_1}-\rho_{e_0e_0}) - \omega_L\rho_{e_{-1}e_1},$$

$$\frac{d}{dt}\rho_{e_{-1}e_1} = -2\gamma\rho_{e_{-1}e_1} + i\Omega\rho^{(+)}_{g_0e_1}e^{-ikz-i\delta t} - i\Omega\rho^{(-)}_{e_{-1}g_0}e^{-ikz+i\delta t} + \omega_L(\rho_{e_0e_1}-\rho_{e_{-1}e_0}). \quad (7)$$

In the above equations the Wigner density-matrix elements have been defined with respect to the time-dependent atomic eigenfunctions. Upper indices stand for the momentum shifts due to the induced transition,

$$\rho^{(\pm)}_{ab} = \langle a|\rho\left(\mathbf{r},\mathbf{p}\pm\tfrac{1}{2}\hbar\mathbf{k}\right)|b\rangle, \quad (8)$$

where $\mathbf{k}=k\mathbf{e}_z$, and the notation $\langle\rho^q_{ll}\rangle$ is adopted for the density-matrix elements averaged over the angular distributions of the spontaneous photon emission [21–26],

$$\langle\rho^q_{ll}\rangle = \int \Phi_q(\mathbf{n})\langle l|\rho(\mathbf{r},\mathbf{p}+\mathbf{n}\hbar k,t)|l\rangle d\mathbf{n}. \quad (9)$$

The function $\Phi_q(\mathbf{n})$ defines the probability of the spontaneous photon emission in the direction of a unit vector $\mathbf{n}$,

$$\Phi_0(\mathbf{n}) = \frac{3}{8\pi}(1-n_z^2), \quad \Phi_{\pm1}(\mathbf{n}) = \frac{3}{16\pi}(1+n_z^2). \quad (10)$$

Rabi frequency and Larmor frequency are defined as

$$\begin{aligned}\hbar\Omega &= \tfrac{1}{2}\langle e_1|d_+|g_0\rangle\mathcal{E} \\ &= -\tfrac{1}{2}\langle g_0|d_-|e_1\rangle\mathcal{E} \\ &= \tfrac{1}{2}\langle e_{-1}|d_-|g_0\rangle\mathcal{E} \\ &= -\tfrac{1}{2}\langle g_0|d_+|e_{-1}\rangle\mathcal{E}, \end{aligned} \quad (11)$$

$$\begin{aligned}\hbar\omega_L &= \tfrac{1}{2}\langle e_1|\mu_+|e_0\rangle\mathcal{B} \\ &= -\tfrac{1}{2}\langle e_0|\mu_-|e_1\rangle\mathcal{B} \\ &= \tfrac{1}{2}\langle e_0|\mu_+|e_{-1}\rangle\mathcal{B} \\ &= -\tfrac{1}{2}\langle e_{-1}|\mu_-|e_0\rangle\mathcal{B}. \end{aligned} \quad (12)$$

The detuning $\delta=\omega_l-\omega_{e_0g_0}$ is the difference between the laser frequency and the atomic transition frequency.

B. Kinetic equation of atomic motion in MOT

In order to follow the Bogolyubov procedure [21–26] we first exclude the explicit time dependence from the density-matrix equations. We perform the substitutions,

$$\rho_{g_0e_\alpha}e^{-i\delta t} = \sigma_{g_0e_\alpha}, \quad (13)$$

where $\alpha=0,\pm1$. Before cooling, it is assumed that the momentum width of the atomic density-matrix elements is much wider than the photon momentum $\hbar k$. Thus the atomic density-matrix elements $\rho_{ij}(\mathbf{r},\mathbf{p}+\hbar\mathbf{k},t)$ can be expanded in the photon momentum $\hbar k$. This principal assumption allows one to expand the density-matrix elements in the power of the photon momentum $\hbar k$. Considering the expanded equations in successively increasing order in the photon momentum $\hbar k$ one can conclude that the diagonal ρ_{aa} and off-diagonal density-matrix elements σ_{ab} are the functionals of the Wigner distribution function $w(\mathbf{r},\mathbf{p},t)$,

$$w(\mathbf{r},\mathbf{p},t) = \rho_{g_0g_0} + \sum \rho_{e_\alpha e_\alpha}. \quad (14)$$

The general structure of the functional dependence can be found directly from the structure of the expanded equations,

$$\rho_{g_0g_0} = \left(\sum_{n=0,\pm2,\ldots} H^n_{g_0g_0} e^{inkz}\right) w + \left(\sum_{n=0,\pm2,\ldots} R^n_{g_0g_0} e^{inkz}\right) \hbar k \frac{\partial w}{\partial p_z} + \cdots, \tag{15}$$

$$\sigma_{g_0e_\alpha} = \left(\sum_{n=1,\pm3,\ldots} H^n_{g_0e_\alpha} e^{inkz}\right) w + \left(\sum_{n=1,\pm3,\ldots} R^n_{g_0e_\alpha} e^{inkz}\right) \hbar k \frac{\partial w}{\partial p_z} + \cdots, \tag{16}$$

$$\rho_{e_\alpha e_\alpha} = \left(\sum_{n=0,\pm2,\ldots} H^n_{e_\alpha e_\alpha} e^{inkz}\right) w + \left(\sum_{n=0,\pm2,\ldots} R^n_{e_\alpha e_\alpha} e^{inkz}\right) \hbar k \frac{\partial w}{\partial p_z} + \cdots, \tag{17}$$

where H^n_{ab} and $R^n_{g_0g_0}$ are functions of the atomic momentum $\mathbf{p}$. Here, in order to exclude the explicit coordinate dependence from the expanded equations, the spatial series representation is introduced. In accordance with the definition of the distribution function $w(\mathbf{r},\mathbf{p},t)$, the unknown diagonal functions satisfy the normalization conditions

$$H^n_{g_0g_0} + H^n_{e_{+1}e_{+1}} + H^n_{e_0e_0} + H^n_{e_{-1}e_{-1}} = \delta_{n,0} \tag{18}$$

and

$$R^n_{g_0g_0} + R^n_{e_{+1}e_{+1}} + R^n_{e_0e_0} + R^n_{e_{-1}e_{-1}} = 0. \tag{19}$$

Next, by taking into account the general structure of the solution, one can see from the expanded equations that the Wigner function $w(\mathbf{r},\mathbf{p},t)$ satisfies the closed equations. To the first order in the photon momentum $\hbar k$, the closed equation for the distribution function can be shown to be the Liouville equation [21–26],

$$\frac{\partial w}{\partial t} + \mathbf{v}\frac{\partial w}{\partial \mathbf{r}} = -\frac{\partial}{\partial p_z}(F_z w), \tag{20}$$

where the radiation force F_z has a series representation as

$$F_z = \hbar k \Omega \sum_{n=0,\pm2,\ldots} f^n_z e^{inkz} \tag{21}$$

and

$$f^n_z = -i(H^{n+1}_{e_1g_0} - H^{n-1}_{g_0e_1}) + i(H^{n-1}_{e_{-1}g_0} - H^{n+1}_{g_0e_{-1}}). \tag{22}$$

Note that the force is defined by a real equation since complex harmonics of the force satisfy the conditions $f^*_n = f_{-n}$, following from the Hermiticity conditions for optical coherence, $H^{n*}_{ab} = H^{-n}_{ba}$. The harmonics $H^n_{g_0g_0}$, $H^n_{e_\alpha e_\beta}$, and $H^n_{e_\alpha e_\alpha}$ satisfy an infinite set of steady-state equations which come from the set of expanded equations considered in zero order in the photon momentum (Appendix A).

To the second order in the photon momentum $\hbar k$ the kinetic equation for the function $w(\mathbf{r},\mathbf{p},t)$ reduces to the Fokker-Planck equation

$$\frac{\partial w}{\partial t} + \mathbf{v}\frac{\partial w}{\partial \mathbf{r}} = -\frac{\partial}{\partial p_z}(F_z w) + \sum \frac{\partial^2}{\partial p_i \partial p_j}(D_{ij} w), \tag{23}$$

where $i,j = x,y,z$ and D_{ij} is the momentum diffusion tensor. The diffusion tensor has the series representation

$$D_{ij} = \hbar^2 k^2 \gamma \sum_{n=0,\pm2,\ldots} d^n_{ij} e^{inkz}. \tag{24}$$

Each spatial harmonic of the diffusion tensor includes two parts,

$$d^n_{ij} = \delta_{iz} d^{dn}_{zz} + d^{an}_{ij}. \tag{25}$$

The first part is that proportional to the optical coherence $R^n_{g_0e_i}$, and can be expressed as

$$d^{dn}_{zz} = i\frac{\Omega}{\gamma}(R^{n+1}_{g_0e_{-1}} - R^{n-1}_{e_{-1}g_0} + R^{n+1}_{e_1g_0} - R^{n-1}_{g_0e_{+1}}). \tag{26}$$

It comes from fluctuations in the number of scattered photons. The second part of the diffusion tensor is proportional to the angular anisotropy coefficients α^σ_{ii}, α^π_{ii}. It originates from fluctuations in the direction of spontaneous photon emission. In this case the coefficients α^σ_{ii} and α^π_{ii} which determine the angular anisotropy of the spontaneous photon emission,

$$\alpha^\sigma_{ii} = \int \Phi_\sigma(\mathbf{n}') n'^2_i d^2n', \quad \alpha^\pi_{ii} = \int \Phi_\pi(\mathbf{n}') n'^2_i d^2n',$$

become

$$\alpha^\sigma_{xx} = \alpha^\sigma_{yy} = \tfrac{3}{10}, \quad \alpha^\sigma_{zz} = \tfrac{2}{5},$$

$$\alpha^\pi_{xx} = \alpha^\pi_{xx} = \tfrac{2}{5}, \quad \alpha^\pi_{zz} = \tfrac{1}{5},$$

and the second part of the diffusion tensor reduces to the approximate expression

$$d^{an}_{ii} = \tfrac{1}{5}(2H^n_{e_1e_1} + H^n_{e_0e_0} + 2H^n_{e_{-1}e_{-1}}). \tag{27}$$

The harmonics of the diffusion tensor satisfy the Hermiticity conditions, $d^{n*}_{ii} = d^{-n}_{ii}$. Steady-state equations of the function R^n_{ab} derived from Eqs. (7) expanded to the first order in the photon momentum are listed in Appendix B.

C. Radiation force, diffusion coefficient, and temperature

Radiation force. As discussed above, to exclude the explicit coordinate dependence, the matrix elements can be expressed as

$$H_{g_0g_0} \equiv H^0_{g_0g_0} + H^{-2}_{g_0g_0} e^{-i2kz} + H^2_{g_0g_0} e^{i2kz} + \cdots,$$

$$H_{g_0e_\beta} \equiv H^{-1}_{g_0e_\beta} e^{-ikz} + H^1_{g_0e_\beta} e^{ikz} + \cdots,$$

$$H_{e_\alpha e_\beta} \equiv H^0_{e_\alpha e_\beta} + H^{-2}_{e_\alpha e_\beta} e^{-i2kz} + H^2_{e_\alpha e_\beta} e^{i2kz} + \cdots. \tag{28}$$

The above decompositions show that the multiphoton process plays an important role in the atom-field interaction. Identification of the processes follows most clearly from the equations considered to different orders of the *rate equation approximation* (REA). As usual, the calculation of atomic functions to the $2n$th order REA implies that the ground- and upper-state populations and coherence are calculated to the $2n$th order REA while the optical coherences are calculated to the $(2n-1)$th order. Considering atomic populations and

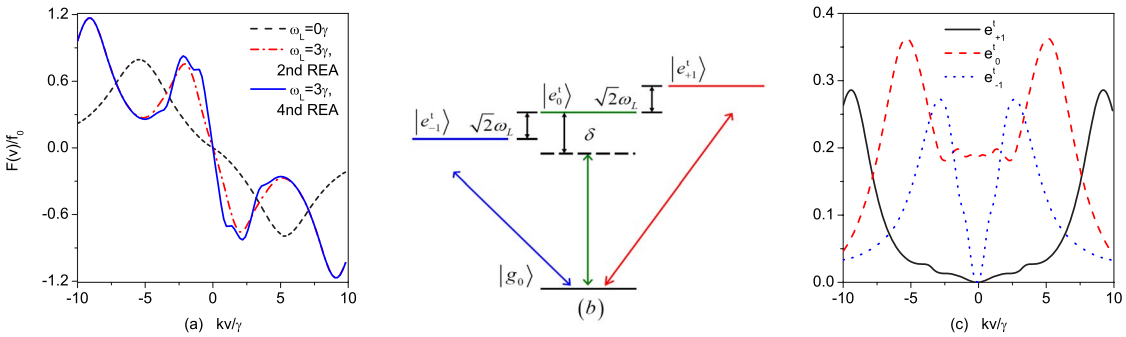

FIG. 2. (Color online) (a) The velocity dependence of the radiation force $F(v)$ calculated to second (dashed-dotted line) and fourth (solid line) order REA with $\Omega=2\gamma$, $\omega_L=0$, 3γ, and $\delta=-5\gamma$. (b) The upper Zeeman sublevels are replaced by the eigenstates $|e^t_{-1,0,1}\rangle$ of $H_B\equiv-\vec{\mu}\mathbf{B}$. (c) The atomic distribution for the eigenstates of $-\vec{\mu}\cdot\mathbf{B}$ with $\Omega=2\gamma$, $\omega_L=3\gamma$, and $\delta=-5\gamma$.

coherences to the second order REA, one takes into account the direct one-photon and two-photon processes and stepwise process composed of the direct processes. When atomic functions are considered to the fourth order REA, one takes into account the direct one-, two-, three-, and four-photon processes, and stepwise processes composed of the above direct process.

By numerically solving the equations listed in Appendix A, we can get the radiation force $F(v)$. Figure 2(a) shows the radiation force $F(v)$ as a function of the atomic velocity v. One could see that the radiation force adding on atoms could be larger than $\hbar k\gamma$, which is the limitation of the two-level Doppler cooling model. It is obvious that another force called stimulated force [13–15] exists in the atom-field interaction. As discussed earlier, σ_+ field can pump atoms from the ground state to the upper Zeeman sublevel $|e_{+1}\rangle$, from which atoms can be transferred to the state $|e_{-1}\rangle$ via Larmor procession and then stimulatively transit back to the ground state by σ_- field. In the whole process, one atom absorbs a reverse propagating photon and stimulatively radiates a copropagating photon. As a result, the change of atomic momentum is $2\hbar k$ in a round trip. With this two-photon process the whole force adding on atoms could be larger than $\hbar k\gamma$ as shown in Fig. 2(a). We also compare the radiation forces including two- and four-photon processes in Fig. 2(a). Below, all figures are calculated up to the four-photon process. Here $f_o=\hbar k\gamma$ is the unit of radiation force.

We should say that this stimulated force has already been studied by Grimm and other workers [13–15]. However, they only considered the interaction of atoms with standing wave by a dressed picture, which gives the dipole force, and they have not shown the final temperature of atoms. The physical model discussed here is different from theirs. In our case, a transverse magnetic field exists in the atom-field interaction system, and atoms interact with $\sigma^+-\sigma^-$ field configuration, not π-π field configuration [14]. Therefore, our cooling physical model is a cooling method, particularly for (1+3)-level alkaline-earth-metal atoms.

At a negative detuning and in a small velocity region the radiation force is reduced to the friction force in the form of

$$F=-\beta v, \tag{29}$$

where $v=v_z$ and β is a friction coefficient, which is defined as the slope of the radiation force near zero velocity. Figure 3(a) shows β changing with the detuning δ for several different Larmor frequencies ω_L. The unit of β is $\beta_o=\hbar k^2$. One can see that the friction coefficient β increases strongly if we introduce the transverse magnetic field $\mathbf{B_t}$. However, since the larger ω_L causes the larger energy shift, β will be negative for large enough $\mathbf{B_t}$, for which atoms will be accelerated, as shown in Fig. 3(a). This could be comprehended by the following physical picture. We could use the eigenstates of $H_B\equiv-\vec{\mu}\cdot\mathbf{B_t}$, which can be expressed as

$$|e^t_{+1}\rangle=\frac{1}{2}|e_{+1}\rangle+\frac{i}{\sqrt{2}}|e_0\rangle-\frac{1}{2}|e_{-1}\rangle,$$

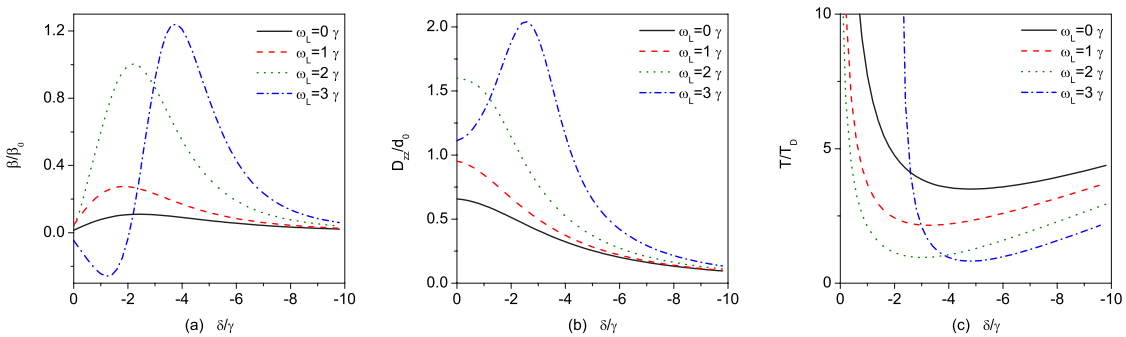

FIG. 3. (Color online) (a) Friction coefficient β of the radiation force as a function of δ and ω_L. (b) The longitudinal diffusion D_{zz} as a function of δ and ω_L. (c) Atomic temperature as a function of δ and ω_L. All curves are calculated in the case $\Omega=2\gamma$.

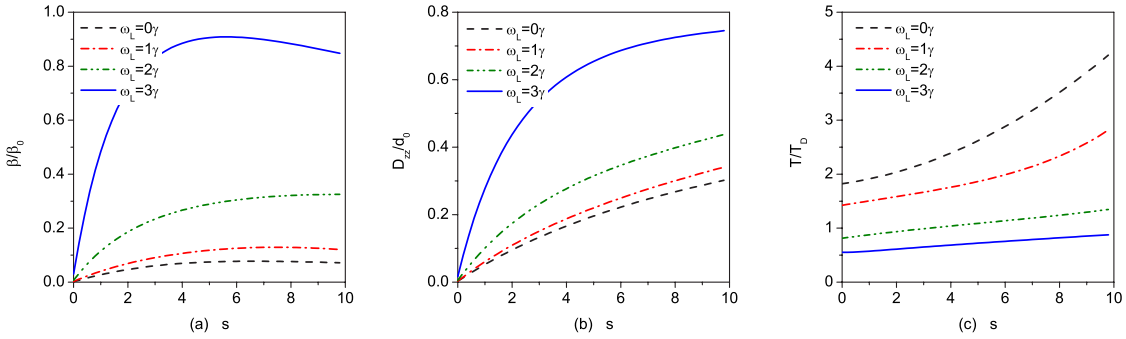

FIG. 4. (Color online) (a) Friction coefficient β of the radiation force as a function of $s=2\frac{\Omega^2}{\gamma^2}$ and ω_L. (b) The longitudinal diffusion D_{zz} as a function of s and ω_L. (c) Atomic temperature as a function of s and ω_L. All curves are at $\delta=-5\gamma$.

$$|e_0^t\rangle = \frac{1}{\sqrt{2}}(|e_{+1}\rangle + |e_{-1}\rangle),$$

$$|e_{-1}^t\rangle = \frac{1}{2}|e_{+1}\rangle - \frac{i}{\sqrt{2}}|e_0\rangle - \frac{1}{2}|e_{-1}\rangle, \tag{30}$$

instead of $|e_{-1,0,+1}\rangle$. The corresponding energy shifts are $\sqrt{2}\hbar\omega_L$, 0, and $-\sqrt{2}\hbar\omega_L$. In this case, the atom-field interaction configuration shown in Fig. 1(b) changes to Fig. 2(b). Thus the upper Zeeman sublevels are no longer degenerate and each level could couple ground state by both σ^+-σ^- fields. Therefore, Fig. 2(b) includes three two-level configurations. However, only two contribute to the radiation force. We show the velocity dependence of atomic distribution among states $|e_{-1,0,+1}^t\rangle$ with the same condition of Fig. 2(a) in Fig. 2(c). Comparing these two figures, one can see that the two apices on either side of $v=0$ (solid line) in Fig. 2(a) correspond to the maxima of populations of $|e_{\pm 1}^t\rangle$ in Fig. 2(c). The atoms on state $|e_0^t\rangle$ do not contribute to the radiation force. The reason is that at position $z=0$, radiation force could be expressed as

$$F_z = i\hbar k\Omega(H_{g_0e_1} + H_{e_{-1}g_0} - H_{e_1g_0} - H_{g_0e_{-1}})$$
$$= i\hbar k\Omega(H_{g_0e_1^t} + H_{g_0e_{-1}^t} - H_{e_1^tg_0} - H_{e_{-1}^tg_0}).$$

We can see that the radiation force is not associated with state $|e_0^t\rangle$. Therefore, atoms on state $|e_0^t\rangle$ do not contribute to the radiation pressure force.

In the limit of small velocity, one can get the analytical result of the friction coefficient β to the second order of REA. Following the method introduced in Ref. [27], the friction coefficient β is given by

$$\beta = \beta_o \frac{4G(-\delta+\sqrt{2}\omega_L)/\gamma}{[1+G+(-\delta+\sqrt{2}\omega_L)^2/\gamma^2]^2}, \tag{31}$$

where $G=\Omega^2/\gamma^2$. From the above expression, one can clearly see that *although the laser detunings of* $|e_{-1,0,1}\rangle$ *are* δ, *the detuning of* $|e_{-1}^t\rangle$ *is* $\delta-\sqrt{2}\hbar\omega_L$ *due to the energy shift caused by transverse magnetic field. Therefore, the radiation force corresponds to detuning* $\delta-\sqrt{2}\hbar\omega_L$, *not* δ. *This is why the radiation force is enhanced strongly.* However, if the energy shift $-\sqrt{2}\hbar\omega_L$ is so large that $\delta-\sqrt{2}\hbar\omega_L<0$, the friction coefficient β will be negative, as show in Fig. 3(b), which means atoms will be accelerated for small detuning δ. This is another physical picture of Fig. 1(b).

Here we should stress that although Fig. 2(b) includes three two-level atom-field configurations, one could not consider the cooling process only using one of them, even in the case of strong magnetic field $\mathbf{B_t}$. This is due to that around $v=0$, the atomic number of state $|e_0^t\rangle$ is not zero. Each of the three two-level atomic systems is not a closed system. There is coherence among three upper Zeeman sublevels. The use of the physical model shown in Fig. 2(b) is to intuitively explain why the fraction coefficient β could be negative in the case of strong magnetic field $\mathbf{B_t}$.

Diffusion coefficient. The next important kinetic quantity that determines the time evolution of an atom in a laser field is the diffusion longitudinal coefficient D_{zz} at position $z=0$. By numerically solving the equations listed in Appendix B, we get the diffusion coefficient D_{zz}. Figure 3(b) shows the velocity dependence of the longitudinal diffusion D_{zz}. The unit of D_{zz} is $d_o=\hbar^2k^2\gamma$. Since D_{zz} is very sensitive to the fluctuations in the number of scattered photons, it will increase as $\mathbf{B_t}$ increases.

Temperatures. Explicit expressions for the coefficients of the Fokker-Planck equations can be directly applied for estimating the achievable temperatures in the scheme of laser cooling of atoms. The effective temperature T is defined by the Einstein relation,

$$T = \frac{D_{zz}(v=0)}{\beta k_B}, \tag{32}$$

where $D_{zz}(v=0)$ is the diffusion coefficient at zero velocity. In Fig. 3(c), we show the temperature as a function of the detuning δ for several different Larmor frequencies ω_L.

The value of atomic temperature crucially depends on the types of optical processes which contribute to the friction and diffusion coefficients. Of the two coefficients, β and D_{zz} $(v=0)$, the most important one is the behavior of the friction coefficient which is very sensitive to the optical processes. Although D_{zz} $(v=0)$ and β both increase if we introduce $\mathbf{B_t}$, β increases more strongly than D_{zz} $(v=0)$. Thus the final temperature could be lower than the usual Doppler temperature, but not much. To express our model more explicitly, we show the temperature changes with the saturation parameter $s=2\frac{\Omega^2}{\gamma^2}$ in Fig. 4.

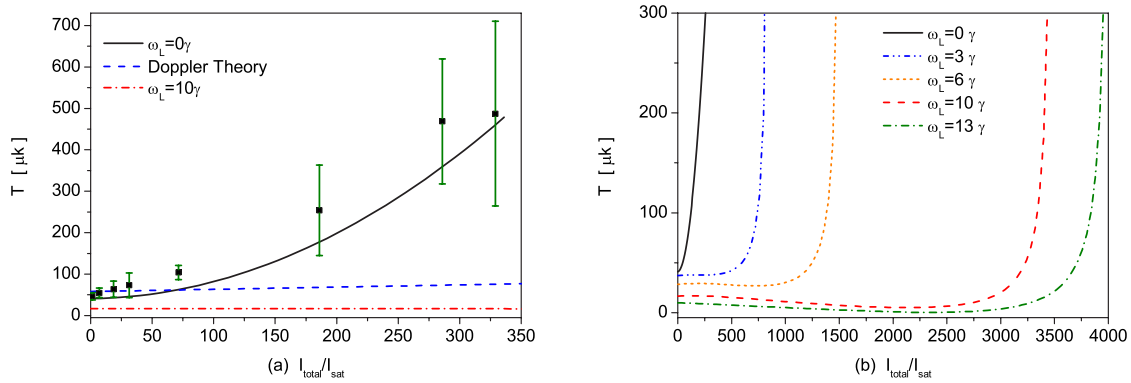

FIG. 5. (Color online) (a) The temperature of ^{174}Yb as a function of $I_{\text{total}}/I_{\text{sat}}$, where $I_{\text{total}}=2I$, I is the intensity of the single field and I_{sat} is the saturation intensity of the transition $(6s^2)^1S_0$-$(6s6p)^3P_1$. Here we also insert the experimental datum of Refs. [30,31], and the temperature calculated by the 1D two-level Doppler cooling theory, which can be expressed as $T=-T_D\frac{\Gamma}{4\delta}(1+\frac{I_{\text{total}}}{I_{\text{sat}}}+4\frac{\delta^2}{\Gamma^2})$, for comparison. The detuning δ here is -13Γ and $\Gamma=2\gamma$. (b) The temperature of ^{174}Yb as a function of $I_{\text{total}}/I_{\text{sat}}$ for several different Larmor frequencies is calculated by our theory.

Example. Recently, Mg, Ca, Sr, and Yb atoms have played significant roles in the field of optical atomic clock. The MOT experimental results of laser cooling of Mg, Ca, Sr, and Yb atoms described by a (1+3)-level atomic model have been compared with the predictions of a one-dimensional (1D) two-level Doppler cooling theory [28–31]. The measured MOT temperature of (1+3)-level atoms, including the even isotope of Mg, Ca, Sr, and Yb, is much higher than the predicted temperature of the two-level atom Doppler cooling theory at high laser intensity [28–31]. Taking the ^{174}Yb atom as the example, for comparison, we set the data of measured ^{174}Yb MOT temperature from Refs. [30,31] in Fig. 5(a). It clearly shows that the measured temperature of ^{174}Yb is significantly higher than expected from 1D two-level Doppler cooling (dashed line). Therefore, one should not calculate the atomic temperature of the (1+3)-level system by the two-level atomic model. As shown in Fig. 5(a), for $\omega_L=0$, our calculation very well agrees with the experimental datum, which could strongly support our model. Moreover, with the existence of transverse magnetic field $\mathbf{B_t}$, the temperature could strongly decrease as the dashed-dotted curve in Fig. 5(a), which will be very useful in experiment. In Fig. 5(b) we show the temperature of ^{174}Yb as a function of $I_{\text{total}}/I_{\text{sat}}$ for several different Larmor frequencies calculated by our theory.

Above all, we have discussed the semiclassical Doppler cooling by the kinetic theory. This theory is only suitable on condition that the momentum width of the atomic density matrix elements exceeds the photon momentum $\hbar k$, for which the atomic density matrix elements $\rho_{ij}(\mathbf{r},\mathbf{p}+\hbar\mathbf{k},t)$ can be expanded in the photon momentum $\hbar k$. However, in the narrow transition line case that the Doppler temperature limit is lower than the recoil limit, the final temperature, that could be reached, is limited by the recoil limit, not the Doppler limit for the narrow transition line [3,4]. Therefore, the semiclassical theory for the model considered above is no longer suitable.

IV. NARROW-LINE LASER COOLING

So far, we have discussed this laser cooling method for (1+3)-level system based on the Fokker-Planck approach. As we have said it is a semiclassical description, which is based on the assumption that the atomic momentum remains constant during the scattering process. For the narrow line, however, the excited-state spontaneous emission rate is comparable to or even smaller than the single-photon recoil frequency. Therefore the semiclassical treatment is not suitable for the narrow line and a full quantum-mechanical treatment should be used.

Here we apply the Monte Carlo (MC) approach to simulate this cooling method for (1+3)-level system for the narrow line. To elucidate the physical manifestation of the cooling, we apply the laser pulses, not cw lasers, to pump atoms stepwise among different levels as shown in Fig. 1(b). The pulses we used here are rectangular waves with width T. To show this more clearly, we take calcium atoms as an example. The narrow cooling line is $(4s4p)^3P_1\leftrightarrow(4s^2)^1S_0$ (wavelength 657 nm), whose linewidth is 0.33 kHz. Here the static magnetic field $\mathbf{B_t}$ is along Oy all of the time, and we assume that all atoms are already precooled by the broad line 423 nm $[(4s4p)^1P_1\leftrightarrow(4s^2)^1S_0]$ to the Doppler limit $T_D=0.83$ mK (42 cm/s), and all atoms are on the ground state initially. As shown in Fig. 6(a), a red-detuned 657 nm pulse comes from the right-hand side and pumps atoms from the ground state onto the upper sublevel state $|e_{-1}\rangle$. After all atoms being transferred from state $|e_{-1}\rangle$ to $|e_{+1}\rangle$ by Larmor procession, a blue-detuned 657 nm pulse comes from the left-hand side to pump atoms back to the ground state by stimulated emission. For symmetry we reverse the above process. Both red and blue detunings are $|\delta_{\text{red/blue}}|=2\pi\times0.23$ MHz. Repeating the above whole procession several times, the temperature of atoms could be closed to the recoil limit as shown below. Following the Jaynes-Cummings (JC) model, the probability that an atom could be pumped onto the excited state by the square pulse with width T can be expressed as

$$P_1=\frac{\Omega^2}{\Omega_G^2}\sin^2\frac{\Omega_G T}{2}, \tag{33}$$

where $\Omega_G^2=\Omega^2+\delta^2$ (this is also the probability for the atom transiting back to the ground state via stimulated emission).

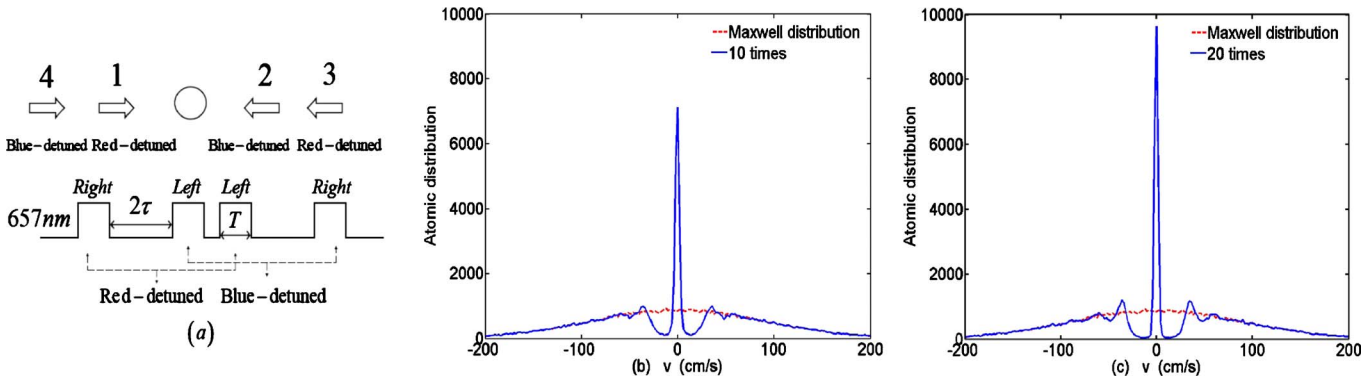

FIG. 6. (Color online) (a) The pulses order in Monte Carlo approach. (b) The atomic momentum distributions after 10 times cooling round trips (Maxwell distribution for dashed line). (c) The atomic momentum distributions after 20 times cooling round trips (Maxwell distribution for dashed line).

One can see from Eq. (33) that the excitation probability will be maximum when $\Omega_G T=\pi$ and is equal to 1 only when the detuning δ is zero. Here we choose the optical intensity 3.6 mW/cm^2, and the duration time of the rectangular pulse is 2.5 μs. Also following the JC model, the probability of magnetic pumping via Larmor procession can be expressed as

$$P_2 = \sin^2 \omega_L \tau. \tag{34}$$

As one can see that all atoms could transit from the one Zeeman sublevel to another sublevel if $\omega_L \tau=\frac{\pi}{2}$, not as Eq. (33), because no Doppler effect is included here. Here we choose the time length of pulse $\tau=2.5$ μs, thus the magnetic field intensity should be $\mathcal{B}=0.07$ G. The interval between two pulses should be 2τ to insure all atoms being transferred from $|e_{+1,-1}\rangle$ to $|e_{-1,+1}\rangle$. Since the lifetime of the metastable state $^3P_1$ is about 400 μs, about 20 times processes can be completed before atoms on the upper levels decay to the ground state. Figures 6(b) and 6(c) show the Monte Carlo results of the cooling method for 10 and 20 times cooling round trips. We assume 10^5 atoms initially. One can see that a high and narrow peak with width of several $\hbar k/m$ exists around the zero velocity in Fig. 6(c).

The use of the transverse magnetic field $\mathcal{B}$ is to transfer the atoms on the upper level from one Zeeman sublevel to another Zeeman sublevel. Therefore, the new force, which is called stimulated force, can act on atoms, and quickly cool atoms down to the recoil limit temperature. This is very useful for narrow-line cooling for alkaline-earth-metal atoms. As discussed in Sec. I, by only using the narrow line, the radiation force is only several times larger than the atomic gravity (especially calcium atoms), for which the cooling process is very slow and atoms could not hold steady in MOT. However, by using the transverse magnetic field $\mathcal{B}$, this can be easily realized. Therefore, the cooling method introduced here will be very useful in experiment. This pulse stimulated cooling method here can also be alternatively and simply realized without $\mathbf{B_t}$, but the field configuration is changed to a single circularly polarized laser field of $\sigma^{\pm}-\sigma^{\pm}$, or $\pi-\pi$ polarization.

Although we only consider the one-dimensional case, this cooling method can be used for the three-dimensional system. One can cool atoms in three dimensions one by one as used in the pulse quenching cooling method [9,10].

V. CONCLUSION

In summary, we have presented a theory of the one-dimension laser cooling for the (1+3)-level atomic system with the help of static transverse magnetic field $\mathbf{B_t}$. Atoms on Zeeman sublevels of the excited state will be redistributed, and the additional stimulated force will be presented in atom-field interaction. Thus the average force adding on atoms are strongly enhanced. For the broad line, the minimum temperature that could be obtained is lower than the Doppler temperature T_D. For the narrow line, the final temperature that can be achieved will be limited by the recoil limit and the average force adding on atoms is much enhanced due to $\mathbf{B_t}$. Therefore the cooling time will be much shorter, and atoms could steadily stay in MOT.

ACKNOWLEDGMENTS

One of the authors (J.C.) thanks E. N. Fortson and R. Maruyama for ^{174}Yb MOT datum, V. G. Minogin and U. Sterr for stimulating discussions, and Ruoxin Li for a critical reading of this paper. This work was supported by MOST of China under Grant No. 2005CB724500 and NSFC under Grant No. 60178016.

APPENDIX A

Below we list an infinite set of linear algebraic equations for the harmonics $H^n_{e_\alpha e_\beta}$, $H^n_{g_0 g_0}$, $H^n_{e_\alpha g_0}$, and $H^n_{g_0 e_\alpha}$. The set of equations originates from set (7) considered to zero order in the photon momentum,

$$H^n_{g_0 g_0} + H^n_{e_{-1} e_{-1}} + H^n_{e_0 e_0} + H^n_{e_{+1} e_{+1}} = \delta_{n,0},$$

$$-2\gamma H^n_{e_1 e_1} - i\Omega(H^{n+1}_{e_1 g_0} - H^{n-1}_{g_0 e_1}) - \omega_L(H^n_{e_0 e_1} + H^n_{e_1 e_0}) - ink\upsilon H^n_{e_1 e_1} = 0,$$

$$-2\gamma H^n_{e_{-1}e_{-1}} - i\Omega(H^{n-1}_{e_{-1}g_0} - H^{n+1}_{g_0e_{-1}}) + \omega_L(H^n_{e_0e_{-1}} + H^n_{e_{-1}e_0}) - inkvH^n_{e_{-1}e_{-1}} = 0,$$

$$-2\gamma H^n_{e_0e_0} - i\Omega(H^n_{e_{-1}e_0} + H^n_{e_0e_{-1}}) + \omega_L(H^n_{e_0e_1} + H^n_{e_1e_0}) - inkvH^n_{e_0e_0} = 0,$$

$$-(\gamma + i\delta)H^n_{g_0e_1} - i\Omega(H^{n+1}_{g_0g_0} - H^{n+1}_{e_1e_1}) + i\Omega H^{n-1}_{e_{-1}e_1} - \omega_L H^n_{g_0e_0} - inkvH^n_{g_0e_1} = 0,$$

$$-(\gamma - i\delta)H^n_{e_1g_0} + i\Omega(H^{n-1}_{g_0g_0} - H^{n-1}_{e_1e_1}) - i\Omega H^{n+1}_{e_1e_{-1}} - \omega_L H^n_{e_0g_0} - inkvH^n_{e_1g_0} = 0,$$

$$-(\gamma + i\delta)H^n_{g_0e_0} + i\Omega H^{n+1}_{e_1e_0} + i\Omega H^{n-1}_{e_{-1}e_0} + \omega_L H^n_{g_0e_1} - \omega_L H^n_{g_0e_{-1}} - inkvH^n_{g_0e_0} = 0,$$

$$-(\gamma - i\delta)H^n_{e_0g_0} - i\Omega H^{n-1}_{e_0e_1} - i\Omega H^{n+1}_{e_0e_{-1}} + \omega_L H^n_{e_1g_0} - \omega_L H^n_{e_{-1}g_0} - inkvH^n_{e_0g_0} = 0,$$

$$-(\gamma + i\delta)H^n_{g_0e_{-1}} - i\Omega(H^{n-1}_{g_0g_0} - H^{n-1}_{e_{-1}e_{-1}}) + i\Omega H^{n+1}_{e_1e_{-1}} + \omega_L H^n_{g_0e_0} - inkvH^n_{g_0e_{-1}} = 0,$$

$$-(\gamma - i\delta)H^n_{e_{-1}g_0} + i\Omega(H^{n+1}_{g_0g_0} - H^{n+1}_{e_{-1}e_{-1}}) - i\Omega H^{n-1}_{e_{-1}e_1} + \omega_L H^n_{e_0g_0} - inkvH^n_{e_{-1}g_0} = 0,$$

$$-2\gamma H^n_{e_{-1}e_0} + \omega_L(H^n_{e_0e_0} - H^n_{e_{-1}e_{-1}}) + i\Omega H^{n+1}_{g_0e_0} + \omega_L H^n_{e_{-1}e_1} - inkvH^n_{e_{-1}e_0} = 0,$$

$$-2\gamma H^n_{e_0e_{-1}} + \omega_L(H^n_{e_0e_0} - H^n_{e_{-1}e_{-1}}) - i\Omega H^{n-1}_{e_0g_0} + \omega_L H^n_{e_1e_{-1}} - inkvH^n_{e_0e_{-1}} = 0,$$

$$-2\gamma H^n_{e_0e_1} + \omega_L(H^n_{e_1e_1} - H^n_{e_0e_0}) - i\Omega H^{n+1}_{e_0g_0} - \omega_L H^n_{e_{-1}e_1} - inkvH^n_{e_0e_1} = 0,$$

$$-2\gamma H^n_{e_1e_0} + \omega_L(H^n_{e_1e_1} - H^n_{e_0e_0}) + i\Omega H^{n-1}_{g_0e_0} - \omega_L H^n_{e_1e_{-1}} - inkvH^n_{e_1e_0} = 0,$$

$$-2(\gamma + i\nu)H^n_{e_1e_{-1}} + i\Omega H^{n-1}_{g_0e_{-1}} - i\Omega H^{n-1}_{e_1g_0} + \omega_L H^n_{e_1e_0} - \omega_L H^n_{e_0e_{-1}} - inkvH^n_{e_1e_{-1}} = 0,$$

$$-2(\gamma - i\nu)H^n_{e_{-1}e_1} - i\Omega H^{n+-1}_{e_{-1}g_0} + i\Omega H^{n-1}_{g_0e_1} + \omega_L H^n_{e_0e_1} - \omega_L H^n_{e_{-1}e_0} - inkvH^n_{e_{-1}e_1} = 0.$$

Integer n denotes the order of the spatial harmonic, $n = 0, \pm 1, \pm 2, \ldots$. Optical coherences H^n_{ab} satisfy the relations: $H^{n*}_{ab} = H^{-n}_{ba}$. When considering only the terms of up to the fourth order in spatial harmonics (fourth order REA), one can obtain 74 linear algebraic equations to be numerically solved.

APPENDIX B

Below we list an infinite set of inhomogeneous algebraic equations for the harmonics $R^n_{e_\alpha e_\beta}$, $R^n_{g_0g_0}$, $R^n_{e_\alpha g_0}$, and $R^n_{g_0e_\alpha}$. The set of equations originates from set (7) considered to first order in the photon momentum,

$$R^n_{g_0g_0} + R^n_{e_{-1}e_{-1}} + R^n_{e_0e_0} + R^n_{e_{+1}e_{+1}} = 0,$$

$$-(2\gamma + inkv)R^n_{e_1e_1} + i\Omega(R^{n+1}_{e_1g_0} - R^{n-1}_{g_0e_1}) + \frac{1}{2}i\Omega(H^{n+1}_{g_0e_1} - H^{n-1}_{e_1g_0}) + \sum_l H^l_{e_1e_1}f^{n-l}_z = 0,$$

$$-(2\gamma + inkv)R^n_{e_{-1}e_{-1}} + i\Omega(R^{n-1}_{e_{-1}g_0} - R^{n+1}_{g_0e_{-1}}) + \frac{1}{2}i\Omega(H^{n-1}_{e_{-1}g_0} - H^{n+1}_{g_0e_{-1}}) + \sum_l H^l_{e_{-1}e_{-1}}f^{n-l}_z = 0,$$

$$-(2\gamma + inkv)R^n_{e_0e_0} + \sum_l H^l_{e_0e_0}f^{n-l}_z = 0,$$

$$-[\gamma + i(\delta + nkv)]R^n_{g_0e_1} - i\Omega(R^{n+1}_{g_0g_0} - R^{n+1}_{e_1e_1}) + i\Omega R^{n-1}_{e_{-1}e_1} - \omega_L H^n_{g_0e_0} + i\Omega\frac{1}{2}(H^{n+1}_{g_0g_0} - H^{n+1}_{e_1e_1}) - i\Omega\frac{1}{2}H^{n-1}_{e_{-1}e_1} + \sum_l H^l_{g_0e_1}f^{n-l}_z = 0,$$

$$-[\gamma - i(\delta - nkv)]R^n_{e_1g_0} + i\Omega(R^{n-1}_{g_0g_0} - R^{n-1}_{e_1e_1}) - i\Omega R^{n-1}_{e_1e_{-1}} - \omega_L H^n_{e_0g_0} - i\Omega\frac{1}{2}(H^{n-1}_{g_0g_0} + H^{n-1}_{e_1e_1}) + i\Omega\frac{1}{2}H^{n+1}_{e_1e_{-1}} + \sum_n H^l_{e_1g_0}f^{n-l}_z = 0,$$

$$-[\gamma + i(\delta + nkv)]R^n_{g_0e_0} + i\Omega R^{n+1}_{e_1e_0} + i\Omega R^{n-1}_{e_{-1}e_0} + i\Omega\frac{1}{2}H^{n+1}_{e_1e_0} - i\Omega\frac{1}{2}H^{n-1}_{e_{-1}e_0} + \sum_l H^l_{g_0e_0}f^{n-l}_z = 0,$$

$$-[\gamma + i(\delta - nkv)]R^n_{e_0g_0} - i\Omega R^{n-1}_{e_0e_1} - i\Omega R^{n+1}_{e_0e_{-1}} - i\Omega\frac{1}{2}H^{n-1}_{e_0e_1} + i\Omega\frac{1}{2}H^{n+1}_{e_0e_{-1}} + \sum_l H^l_{e_0g_0}f^{n-l}_z = 0,$$

$$-[\gamma+i(\delta+nkv)]R^n_{g_0e_{-1}}-i\Omega(R^{n-1}_{g_0g_0}-R^{n-1}_{e_{-1}e_{-1}})+i\Omega R^{n+1}_{e_1e_{-1}}+\omega_L H^n_{g_0e_0}-i\Omega\frac{1}{2}(H^{n-1}_{g_0g_0}+H^{n-1}_{e_{-1}e_{-1}})+i\Omega\frac{1}{2}H^{n+1}_{e_1e_{-1}}+\sum_l H^l_{e_0e_0}f_z^{n-l}=0,$$

$$-[\gamma-i(\delta-nkv)]R^n_{e_{-1}g_0}+i\Omega(R^{n+1}_{g_0g_0}-R^{n+1}_{e_{-1}e_{-1}})-i\Omega R^{n-1}_{e_{-1}e_1}+\omega_L H^n_{e_0g_0}+i\Omega\frac{1}{2}(H^{n+1}_{g_0g_0}+H^{n+1}_{e_{-1}e_{-1}})-i\Omega\frac{1}{2}H^{n-1}_{e_1e_{-1}}+\sum_l H^l_{e_0e_0}f_z^{n-l}=0,$$

$$-(2\gamma+inkv)R^n_{e_{-1}e_0}+i\Omega R^{n+1}_{g_0e_0}+i\Omega\frac{1}{2}H^{n+1}_{g_0e_0}+\sum_l H^l_{e_{-1}e_0}f_z^{n-l}=0,$$

$$-(2\gamma+inkv)R^n_{e_0e_{-1}}-i\Omega R^{n-1}_{e_0g_0}-i\Omega\frac{1}{2}H^{n-1}_{e_0g_0}+\sum_l H^l_{e_0e_{-1}}f_z^{n-l}=0,$$

$$-(2\gamma+inkv)R^n_{e_0e_1}-i\Omega R^{n+1}_{e_0g_0}+i\Omega\frac{1}{2}H^{n+1}_{e_0g_0}+\sum_l H^l_{e_0e_1}f_z^{n-l}=0,$$

$$-(2\gamma+inkv)R^n_{e_1e_0}+i\Omega R^{n-1}_{g_0e_0}-i\Omega\frac{1}{2}H^{n-1}_{g_0e_0}+\sum_l H^l_{e_1e_0}f_z^{n-l}=0,$$

$$-2\left(\gamma+i\frac{n}{2}kv\right)R^n_{e_{-1}e_1}-i\Omega R^{n+1}_{e_{-1}g_0}+i\Omega R^{n+1}_{g_0e_1}+i\Omega\frac{1}{2}H^{n+1}_{e_{-1}g_0}+i\Omega\frac{1}{2}H^{n+1}_{g_0e_1}+\sum_l H^l_{e_{-1}e_1}f_z^{n-l}=0,$$

$$-2\left(\gamma+i\frac{n}{2}kv\right)R^n_{e_1e_{-1}}+i\Omega R^{n-1}_{g_0e_{-1}}-i\Omega R^{n-1}_{e_1g_0}-i\Omega\frac{1}{2}H^{n-1}_{g_0e_{-1}}-i\Omega\frac{1}{2}H^{n-1}_{e_1g_0}+\sum_l H^l_{e_1e_{-1}}f_z^{n-l}=0.$$

The above set can be solved when the inhomogeneous terms have been determined from the solution of the set of equations listed in Appendix A.

[1] W. D. Phillips *et al.*, J. Opt. Soc. Am. B **6**, 2084 (1989).
[2] J. Dalibard and C. Cohen-Tannoudji, J. Opt. Soc. Am. B **6**, 2023 (1989).
[3] P. J. Ungar, D. S. Weiss, E. Riis, and S. Chu, J. Opt. Soc. Am. B **6**, 2058 (1989).
[4] D. S. Weiss, E. Riis, Y. Shevy, P. J. Ungar, and S. Chu, J. Opt. Soc. Am. B **6**, 2072 (1989).
[5] Y. Castin, H. Wallis, and J. Dalibard, J. Opt. Soc. Am. B **6**, 2046 (1989).
[6] H. Wallis and W. Ertmer, J. Opt. Soc. Am. B **6**, 2211 (1989).
[7] K. R. Vorgel, T. P. Dineen, A. Gallagher, and J. L. Hall, IEEE Trans. Instrum. Meas. **48**, 618 (1999).
[8] T. Binnewies, G. Wilpers, U. Sterr, F. Riehle, J. Helmcke, T. E. Mehlstaubler, E. M. Rasel, and W. Ertmer, Phys. Rev. Lett. **87**, 123002 (2001).
[9] E. A. Curtis, C. W. Oates, and L. Hollberg, Phys. Rev. A **64**, 031403(R) (2001).
[10] T. E. Mehlstaeubler, J. Keupp, A. Douillet, N. Rehbein, E. M. Rasel, and W. Ertmer, J. Opt. B: Quantum Semiclassical Opt. **5**, S183 (2003).
[11] A. P. Kazantsev, Sov. Phys. JETP **39**, 784 (1974).
[12] V. S. Voitsekhovich, M. V. Danileiko, A. M. Negrijko, V. I. Romanenko, and L. P. Yatsenko, Sov. Phys. Tech. Phys. **33**, 690 (1988).
[13] R. Grimm, Yu. B. Ovchinnikov, A. I. Sidorov, and V. S. Letokhov, Phys. Rev. Lett. **65**, 1415 (1990).
[14] J. Söding and R. Grimm, Phys. Rev. A **50**, 2517 (1994).
[15] J. Söding, R. Grimm, Yu. B. Ovchinnikov, Ph. Bouyer, and Ch. Salomon, Phys. Rev. Lett. **78**, 1420 (1997).
[16] R. Kaiser, N. Vansteenkiste, A. Aspect, E. Arimondo, and C. Cohen-Tannoudji, Z. Phys. D: At., Mol. Clusters **18**, 17 (1991).
[17] B. Sheehy, S.-Q. Shang, P. van der Straten, S. Hatamian, and H. Metcalf, Phys. Rev. Lett. **64**, 858 (1990).
[18] S.-Q. Shang, B. Sheehy, P. van der Straten, and H. Metcalf, Phys. Rev. Lett. **65**, 317 (1990).
[19] G. Nienhuis, P. Y. van der Straten, and S.-Q. Shang, Phys. Rev. A **44**, 462 (1991).
[20] H. J. Metcalf and P. van der Straten, *Laser Cooling and Trapping* (Springer, New York, 1999).
[21] S. Chang, T. Y. Kwon, H. S. Lee, and V. G. Minogin, Phys. Rev. A **64**, 013404 (2001).
[22] S. Chang and V. Minogin, Phys. Rep. **365**, 65 (2002).
[23] V. G. Minogin and V. S. Letokov, *Laser Light Pressure on Atoms* (Gordon and Breach, New York, 1987).
[24] S. Chang, T. Y. Kwon, H. S. Lee, and V. Minogin, Phys. Rev. A **60**, 2308 (1999).
[25] J. W. Jun, S. Chang, T. Y. Kwon, H. S. Lee, and V. G. Minogin, Phys. Rev. A **60**, 3960 (1999).
[26] S. Chang, T. Y. Kwon, H. S. Lee, and V. G. Minogin, Phys. Rev. A **60**, 3148 (1999).
[27] Daniel J. Phalen, Colin C. Young, Su Yi, and Han Pu, Phys. Rev. A **72**, 033406 (2005).
[28] X. Xu, T. H. Loftus, M. J. Smith, J. L. Hall, A. Gallagher, and J. Ye, Phys. Rev. A **66**, 011401(R) (2002).
[29] X. Xu, T. H. Loftus, J. L. Hall, A. Gallagher, and J. Ye, J. Opt. Soc. Am. B **20**, 968 (2003).
[30] R. Maruyama, R. H. Wynar, M. V. Romalis, A. Andalkar, M. D. Swallows, C. E. Pearson, and E. N. Fortson, Phys. Rev. A **68**, 011403(R) (2003).
[31] R. Maruyama, Ph.D. thesis, University of Washington, 2003.